Environmental Science and Pollution Research (2019) 26:36124–36140
https://doi.org/10.1007/s11356-019-06607-8

REVIEW ARTICLE

Overview performance of lanthanide oxide catalysts in methanation reaction for natural gas production

Salmiah Jamal Mat Rosid[1] · Susilawati Toemen[2] · Malik Muhammad Asif Iqbal[2] · Wan Azelee Wan Abu Bakar[2] · Wan Nur Aini Wan Mokhtar[3] · Md Maniruzzaman A. Aziz[4]

Received: 18 November 2018 / Accepted: 24 September 2019 / Published online: 20 November 2019

Abstract

A rapid growth in the development of power generation and transportation sectors would result in an increase in the carbon dioxide (CO_2) concentration in the atmosphere. As it will continue to play a vital role in meeting current and future needs, significant efforts have been made to address this problem. Over the past few years, extensive studies on the development of heterogeneous catalysts for CO_2 methanation have been investigated and reported in the literatures. In this paper, a comprehensive overview of methanation research studies over lanthanide oxide catalysts has been reviewed. The utilisation of lanthanide oxides as CO_2 methanation catalysts performed an outstanding result of CO_2 conversion and improvised the conversion of acidity from CO_2 gas to CH_4 gas. The innovations of catalysts towards the reaction were discussed in details including the influence of preparation methods, the structure-activity relationships as well as the mechanism with the purpose of outlining the pathways for future development of the methanation process.

Keywords Lanthanide oxide · Catalyst · Mechanism · Carbon dioxide · Methanation · Natural gas

Highlights
- The current technologies used in natural gas to reduce the emission of greenhouse gases have been discussed.
- This paper focused on the potential usage of lanthanide elements as a catalyst in methanation reaction.
- Importance of pathway mechanism in methanation reaction to identify the intermediate species and final product obtained has been considered.

Responsible editor: Philippe Garrigues

✉ Salmiah Jamal Mat Rosid
salmiahjamal@unisza.edu.my

✉ Susilawati Toemen
susilawatitoemen@utm.my

[1] Unisza Science and Medicine Foundation Centre, Universiti Sultan Zainal Abidin, Gong Badak Campus, 21300 Kuala Nerus, Terengganu, Malaysia

[2] Department of Chemistry, Faculty of Science, Universiti Teknologi Malaysia (UTM), 81310 Skudai, Johor, Malaysia

[3] Centre for Advanced Materials and Renewable Resources, Faculty of Science & Technology, Universiti Kebangsaan Malaysia, 43600 Bangi, Selangor, Malaysia

[4] Faculty of Civil Engineering, Universiti Teknologi Malaysia (UTM), 81310 Skudai, Johor, Malaysia

Nomenclatures

AC	Activated carbon
Ar	Argon
atm	Atmosphere
Ba	Barium
C_2H_6	Ethane
Ce	Cerium
CH_4	Methane
Cl	Chlorine
CO	Carbon monoxide
Co	Cobalt
CO_2	Carbon dioxide
Cu	Copper
FTIR	Fourier transform infrared
GHGs	Greenhouse gases
GHSV	Gas hourly space velocity
h	Hour
H_2	Hydrogen
H_2S	Hydrogen sulphide
HRTEM	High-resolution transmission electron microscopy
K	Potassium
La	Lanthanum
LOs	Lanthanide oxides
Mg	Magnesium

Mn	Manganese
Mo	Molybdenum
MS	Mass spectroscopy
N_2	Nitrogen
Ni	Nickel
NO	Nitrogen monoxide
Pa	Pascal
Pd	Palladium
Pr	Praseodymium
PSA	Pressure swing adsorption
Rh	Rhodium
Ru	Ruthenium
Sm	Samarium
SO_2	Sulphur dioxide
Sr	Strontium
TEM	Transmission electron microscopy
TPR	Temperature-programmed reduction
UNFCCC	United Nations Framework Convention on Climate Change
XPS	X-ray photoelectron spectroscopy
XRD	X-ray diffraction

Introduction

Nowadays, demands on natural gas have been increased as the second largest worldwide energy (Khan 2015; Dong et al. 2017; Curry 1981). Natural gas is the most essential source in daily usage as it promises less harmful by-products into the air and considered as the cleanest and safest to the environment (Solarin and Ozturk 2016; Kakaee et al. 2014; Aleman-Nava et al. 2014). However, the quality of natural gas is disputed due to the presence of unwanted compounds such as non-associated gases including carbon dioxide (CO_2). According to Speight (2007), these impurities formed corrosive compound, for example carbonic acid in the presence of water, and thus corroded the pipeline of natural gas, reducing the quality and value of natural gas due to its sour properties in worldwide markets as well as causing difficulties for its distribution to the market.

On the other hand, air pollution is also being affected by the high CO_2 content released into the atmosphere. Some effects of the escalating concentration in greenhouse gases (GHGs) within the atmosphere are global warming, which seems to be an invisible threat to humans. Hence, the establishment of the United Nations Framework Convention on Climate Change (UNFCCC) emphasised on stabilising GHG concentration at permissible level so as to protect the climatic stance from deleterious factors (Strakey et al. 1975). In fact, the term 'carbon credit' was implemented to control the commercial and industrial sectors to cut the release of excessive CO_2 or GHGs into the environment. As a consequence, the necessity of green technology is unquestionable to minimise GHG emission, particularly involving fossil fuels.

Among technologies used, catalytic methanation reaction is widely explored to convert CO_2 in natural gas into methane (CH_4) for the effective and complete combustion. Some of potential catalysts, i.e. nickel, cobalt, iron and copper, expressed a good performance towards methanation reaction (Bakar et al. 2012; Bakar et al. 2012; Zamani et al. 2015a, b). However, among catalysts prepared for this particular purpose, lanthanide oxides (LOs) are noteworthy candidates to convert CO_2 gas and are promising higher selectivity towards methane species. Up to date, a comprehensive study in natural gas to simultaneously convert CO_2 to CH_4 in industry by reducing emission of impurities by-products has not been conducted using lanthanide oxide. Lanthanide oxide, the unique properties of this metal oxide to among other elements, was particularly in oxidation state. LOs that existed in their trivalent state possessed higher-degree stabilisation in 4*f*, 5*d* and 4*s* orbitals upon ionisation and provided basic catalyst, which took them to stand out as the most versatile materials for methanation reaction. Other than that, the number of unpaired electron could be seven, whereby enhancing a large magnetic moment in chemical bond (Curry 1981). Taking these into account, therefore, this review paper aims to provide an idea on the advantage of LOs in catalytic methanation to produce higher-quality natural gas. In addition, this paper also focused on the compilation of a wide range of lanthanide oxide elements and their functions as a based promoter, co-catalyst and support. It is also purposely to grab the attention of researchers to explore on other lanthanide oxides through reasonable and systematic method catalytic methanation. Table 1 summarises the benefits and drawbacks of lanthanide oxide.

Herein, this paper has fulfilled the gap by discussing more on the lanthanide oxides, i.e. lanthanum (La), cerium (Ce), praseodymium (Pr) and samarium (Sm) catalysts, to convert CO_2 into methane gas. This article is organised as follows: the section "Current technologies in methanation reaction" reports the overview of technologies used in natural gas, while the section "Methanation catalysts" reviews the existing literature on CO_2 methanation catalysts as well as in-depth deal with the performance of lanthanide oxide catalysts. The section "Physicochemical properties of lanthanide oxide catalysts through characterisation analyses" presents the physicochemical properties of lanthanide oxide catalysts, while the section "Mechanism of catalytic CO_2 methanation reaction" discusses the mechanistic study of methanation catalyst; finally, the section "Conclusion and future aspect" presents concluding remarks and a perspective outlook for future works.

Table 1 Some of the benefits and drawbacks of lanthanide oxide

Benefits of lanthanide oxide	Drawbacks of lanthanide oxide
LOs as a based catalyst:	LOs as a promoter, co-catalyst and support:
i. Provided higher CO_2 conversion after promoted by manganese and ruthenium oxides	i. The CO_2 conversion is lower
ii. Higher purity of natural gas by greater CH_4 formation	ii. Achieved lower CH_4 formation
iii. Mechanistic study showed a direct dissociation of CO_2 to CH_4 without formation of carbon monoxide, carbonate and formate	iii. Mechanistic study showed formation of a few intermediates such as carbon monoxide, carbonate and formate

Current technologies in methanation reaction

Increment of standard and purified natural gas production appears to be liaised with its escalating demand. It is absolutely necessary to discard CO_2 and hydrogen sulphide in generating sweet natural gas to ascertain clean burning and safety for the environment. The pressure swing adsorption (PSA) measure was commonly employed to purify gases by pushing the pressure to the down level. This particular process can be applied to discard CO_2 from streams of highly pressured gases based on species molecular and affinity for an adsorbent material (Haldor Topsøe 2005; Riboldi and Bolland 2017). Additionally, the process of amine sweetening can also eliminate the pollutants to generate clean gases that were fitted for transportation purposes (William and David 2005).

Moreover, the gas scrubber (Michael et al. 2010; Stookey et al. 1986) and the water scrubber (Biernat and Gisw 2012) technologies were currently used by applying the Prism membrane to remove CO_2 in order to adhere to the specification of pipelines and enhanced the value of heating for gas. The membrane separated CO_2 efficiently from hydrocarbon vapours at a lower temperature, mainly because of its solubility aspect higher than methane. Upon dissolving CO_2 in water, the concentration of methane within the gas phase was increased at the scrubber column (Biernat and Gisw 2012). This process of separating membrane was carried out to permeate selected gases, such as CO_2, H_2 and H_2S, which appear to be part of the permeated gas in the membrane, thus diffused through the material of the membrane (Zuo et al. 2014). The membrane module has been reported to escalate the process of permeation in components with higher permeation rates (Aasberg-Petersen et al. 2011), in comparison to those components that suggested permeation at a lower rate, for instance N_2, Cl, C_2H_6 and heavier hydrocarbons.

Another method that has been widely used in industry to treat sour gas referred to the iron sponge process (Anerousis and Whitman 1984), which was a simple yet effective approach in applications related to systems with low pressure, natural gas with high pressure as well as sewerage gas from sewer sludge as a result of anaerobic digestion (Abdulrahman and Sebastine 2012). However, all of the mentioned technologies spoiled a few shortcomings such as not easily adapted to continuous operating cycle, incurred high fuel cost and dependent on operating conditions of the feed gas.

Therefore, years by years, catalytic chemical conversion has become a more promising technique to remove CO_2 and H_2S gases (Wan Abu Bakar et al. 2015). This method has the ability to enhance the purity of the natural gas by simultaneously converting them to methane gas using heterogeneous catalysts (Habazaki et al. 1998; Silva et al. 2012; Hoekman et al. 2010; Liu et al. 2012a, b; Munik et al. 2014; Brooks et al. 2007; Beuls et al. 2012; Djinovic et al. 2011; Abe et al. 2009; Zamani et al. 2014). Catalytic methanation reaction has received great attention due to its economical approach as these catalysts may be regenerated, reused and safe for the environment because no harmful gas was emitted into the environment at the reaction time. However, the most challenging factor for this technology was to achieve this reaction under mild conditions due to kinetic barriers. Consequently, the development of proper catalysts to lower the activation energy of methanation reaction was critical as how they worked in reaction as will be discussed in the section "Methanation catalysts". Table 2 summarises the current technologies used in processing natural gas.

Methanation catalysts

In general, the methanation reaction is the catalytic reactions that convert CO_2 or carbon monoxide into methane and water products when reacting with hydrogen as described in Eqs. (1) and (2). This reaction is also called a Sabatier reaction with moderately exothermic value of $\Delta H = -165$ kJ mol^{-1} and is dependent on the interfaces of active sites and the reactions through adsorption-desorption at the catalyst surface (Saluko 2005).

$$CO_{2(g)} + 4H_{2(g)} \rightarrow CH_{4(g)} + 2H_2O_{(l)} \quad (1)$$

$$CO_{(g)} + 3H_{2(g)} \rightarrow CH_{4(g)} + H_2O_{(l)} \quad (2)$$

Typically, the selection of active catalyst applied in CO_2 methanation considered higher basicity in accordance with CO_2 acidity, as well as higher surface area with dispersion of smaller-sized particles upon the surface of the catalyst. It has been found that metal oxides were the most significant and

Table 2 Summarisation of current technologies in processing natural gas

Process	Function	Advantages	Disadvantages	Ref
Iron sponge process	H_2S removal and the one that leaves the CO_2 in the natural gas	Effective for high-pressure natural gas, sewerage gas from anaerobic digestion of sewer sludge	Batch-type function and not easily adapted to continuous operating cycle and effectiveness of iron oxide not lasting forever	Curry 1981; Anerousis and Whitman 1984; Abdulrahman and Sebastine 2012
Polymer membranes	To reduce the concentration of CO_2 and H_2S in the natural gas to US pipeline specifications	Minimal maintenance cost, no involvement of hazardous chemical and easy to be operated	Incurs high fuel cost, highly dependent on CO_2 content and low selectivity towards toxic gas separation	Biernat and Gisw 2012
Chemical absorption processes	Aqueous alkanolamine solutions are used for treating gas streams containing H_2S and CO_2	Lower installation and removal costs	Good reactivity at low cost and good flexibility in design and operation but depending on the composition and operating conditions of the feed gas	Michael et al. 2010; Stookey et al. 1986; Mokhatab et al. 2006
Pressure swing adsorption	Remove CO_2 from high-pressure gas streams	No hazardous chemical involved (activated carbon and zeolite only)	Deactivation of the bed will occur when adsorption of H_2S and H_2O occurs on activated carbon	Haldor Topsøe 2005; William and David 2005
Chemical conversion techniques	Conversion of CO_2 gas to produce methane	Using catalyst, inexpensive and increase CH_4 formation	–	Bakar et al. 2015; Habazaki et al. 1998; Silva et al. 2012; Hoekman et al. 2010; Liu et al. 2012; Munik et al. 2014; Brooks et al. 2007; Beuls et al. 2012; Djinovic et al. 2011; Abe et al. 2009; Zamani et al. 2014

commonly employed catalysts for its exceptional ability in transferring electron and proton, besides generating redox reactions with the assistance of catalyst support dispersion which stabilises the catalytic aspect of the active species (Seiyama 1992). For instance, nickel, an element in group VIII metals, was a conventional catalyst applied in the industrial sector (Bakar et al. 2009) in the form of metal oxide. Although it generated an enhanced reaction, its drawback lied in the severe carbon deposition at higher reaction temperature. On the other hand, for ruthenium and rhodium, both exhibited greater results with higher CO_2 conversion but still were costly and scarcely available for a giant scale of operation (Akin et al. 2002).

Second drawback related to high CO_2 methanation was unable to deal with sole metal oxides. However, the improvement in stability and activity can be accounted by an electronic modification which resulted from the direct bonding or from structural change induced by one metal upon the other via the contribution of promoter or co-catalyst metal oxides (Tang et al. 2006). It was also fair to state that the development of mixed metal oxide as a catalyst was much slower due to its multiple oxidation states, variable local coordination, coexisting bulk and varied surface termination functionalities (Ertesva et al. 2005). There were a number of research studies previously reported in gaining excellent catalyst that can contribute higher activity of CO_2 methanation reaction. Several methanation catalysts had been evidently patented and are tabulated in Table 3.

Overall, the lack of report about lanthanide oxide catalysts in methanation reaction was found. Under the circumstances, the most applied LO elements in methanation reaction were Ce and La.

Ideally, lanthanide oxide catalysts mostly would affect the chemical modification of catalysts as well as catalytic activity and stability in CO_2 hydrogenation (Feng et al. 2014). Generally, lanthanide series that were used as catalysts was lanthanum, cerium, samarium and praseodymium. In pioneering research studies by Song et al. (2010), La_2O_3 commonly acted as an electronic modifier in Ni catalysts due to its good dispersion of hexagonal crystalline structure on the surface for charge trapping. The 10% Ni/La_2O_3 showed an excellent activity towards CO_2 methanation and displayed an important activity at low temperature (280 °C) to produce CH_4. Meanwhile, a significant improvement in the stability and high-temperature steam resistance was also observed over a Ni/Al_2O_3 catalyst doped with lanthanum oxide (Su and Guo 1999; Wierzbicki et al. 2016). The addition of rare-earth oxides has suppressed the growth of Ni particle, the oxidation of active component Ni and the formation of $NiAl_2O_4$ species, thus significantly reducing the catalyst deactivation. On the other hand, lanthanum oxide was also used as a dopant in Ru impregnated on alumina. The results obtained showed that the reaction temperature was approximately lowered by 30 °C

Table 3 Patented methanation catalyst

Patent no.	Inventor	Catalyst	Characteristic features
8,658,554	Dorner et al. (2014)	Cerium, lanthanum	Preparation method: impregnation Temperature = 200–450 °C Pressure = 0.5–5 MPa CH_4 yield: –
8,629,077	Li (2014)	Lanthanum, cerium supported alumina	Preparation method: co-precipitation Temperature = 80–350 °C Pressure = 1–5 atm CH_4 yield: –
8,754,137	Scholten et al. (2012)	Nickel-chromium	Preparation method: sol-gel Temperature = 205–220 °C Pressure = 450 psig CH_4 yield = 100%
20,100,168,257	Duissberg et al. (2010a, b)	Nickel	Preparation method: sol-gel Temperature = 160–340 °C Pressure = 1–5 atm CH_4 yield = > 80%
02,010,006,386	Ruiz et al. (2009)	Ruthenium	Preparation method: impregnation Temperature = 150 °C Pressure = 10^4 Pa CH_4 yield = 100%
02008/110331	Duisberg et al. (2008)	Nickel	Preparation method: impregnation Temperature = 180–270 °C Pressure = 1–5 atm CH_4 yield = > 75%
7,071,239	Ortego et al. (2006)	Cobalt, magnesium, zirconium, boron, aluminium, baron, silicon and lanthanum	Preparation method: impregnation Temperature = 160–300 °C Pressure = 1–10 atm CH_4 yield: –
8,067,332	Lee et al. (2006)	Platinum, ruthenium, cobalt, nickel	Preparation method: impregnation Temperature = 200 °C Pressure: – CH_4 yield: –
000/16901	Henville (2000)	Nickel oxide doped yttrium oxide	Preparation method: impregnation Temperature = 250–550 °C Pressure = 100–500 kPa CH_4 yield = > 50%
4,666,881	Wood and Gleason (1987)	Ruthenium supported on oxide of tantalum, niobium, vanadium or their mixtures	Preparation method: impregnation Temperature = 250–350 °C Pressure = 1–5 atm CH_4 yield = 86.5%
4,368,142	Frohning and Horn (1983)	Supported nickel, cobalt and magnesium	Preparation method: impregnation Temperature = 300–600 °C Pressure = 10–80 atm CH_4 yield = 58.3%
4,196,100	Pargeter and Ahmad (1980)	Nickel oxide	Preparation method: fluid bed roasting Temperature = 315–425 °C Pressure = 800 psig CH_4 yield = 86%
4,168,276	Finch (1979)	Copper-molybdenum	Preparation method: impregnation Temperature = 450–550 °C Pressure = 100–2000 psig CH_4 yield = 44.2%
4,260,553	Happel and Hnatow (1979)	Molybdenum, lanthanum	Preparation method: impregnation Temperature = 300–600 °C Pressure = 100–2000 psig CH_4 yield = 58%
3,988,334	Finch and Ripley (1976)	Supported nickel or cobalt promoted noble metals	Preparation method: impregnation Temperature = 275–350 °C Pressure = 0–12,000 psig CH_4 yield = 89.9%
3,947,483	Kobylinski and Swift (1976)	Metal chrysotile	Preparation method: impregnation Temperature = 204–816 °C Pressure = 1–1000 atm CH_4 yield = 96.3% after 10 h

compared to pure Ru/Al_2O_3 (Chen et al. 2007). The CO conversion and selectivity for $Ru\text{-}La_2O_3/Al_2O_3$ was above 99% in the presence of hydrogen-rich gas at temperature above 200 °C. Meanwhile, the incorporation of optimum 5 wt% Ru into $Co/La/Al_2O_3$ also has been investigated by Rosid et al. (2015b) which gave almost 100% of CO_2 conversion with 43.40% of CH_4 formation when the reaction temperature achieved was 300 °C.

Cerium, a commercial lanthanide element has been vastly examined due to its stronger redox ability and larger surface area (62.6 nm) (Fred 2008; Sims et al. 2019). The basicity of cerium could escalate the adsorption of CO_2 at the surface of the catalyst, while its exceptional redox ability derives from the oxygen vacancies formed at its surface due to the rapidly decreasing Ce^{4+}/Ce^{3+} (Rao and Mishra 2003; Centi et al. 2013; Boaro et al. 2019). Cerium oxide catalyst was also applied in NO and SO_2 reduction reaction due to its stability without being deactivated by these gases. Meanwhile, the performance of bimetallic Co/Ce oxide catalyst was investigated by Arsalanfar et al. (2012) using a co-precipitation method for Fischer-Tropsch synthesis. The 60 wt% of ceria (Co/Ce, 40:60) was the optimum catalyst ratio for CO methanation reaction whereby it gave 90% conversion and 45% methane selectivity. By reducing the content of Ce to 50 wt% (Co/Ce, 50:50), the conversion obtained was similar as 60 wt% but slightly lower in their methane selectivity (35%) due to the increment of Co_3O_4 species (Xu et al. 2006). Furthermore, Sharma et al. (2011) also have investigated that Ru-doped ceria, $Ce_{0.95}Ru_{0.05}O_2$, showed higher CO_2 conversion and CH_4 selectivity with 55% and 99%, respectively, at 450 °C by the ratio CO_2:H_2:Ar (13:54:33) at the gas hourly space velocity (GHSV) of 10,000 h^{-1}.

A simple technique of impregnation was applied for the preparation of Ru/cerium oxide $(CeO_2)/Al_2O_3$, with Ru loading of 2% by weight with Ce as a based catalyst (Tada et al. 2014). As expected, the $Ru/CeO_2/Al_2O_3$ catalyst showed higher catalytic activity of methanation than CeO_2/Al_2O_3 and Ru/Al_2O_3. Selectivity methane formation of $Ru/CeO_2/Al_2O_3$ was greater than that of Ru/CeO_2. Cerium oxide could also be recognised as a promoter (Jenewein et al. 2003) for CO_2 hydrogenation. The addition of 2 wt% Ce towards a Ni-based catalyst by impregnation method was done by Liu et al. (2012a, b). They found that the incorporating of Ce had promoted CO_2 adsorption on the Ni-2% CeO_2/Al_2O_3 catalyst surface and caused CO_2 conversion increased to 71% with 99% selectivity to methane gas. Meanwhile, the Ni/Al_2O_3 catalyst just achieved 45% CO_2 conversion with 99% CH_4 selectivity. Both catalysts were tested at a reaction temperature of 300 °C, with a ratio of 4:1 (CO_2:H_2) and GHSV of 15,000 mL g^{-1} h^{-1}.

In addition, Xavier et al. (1999) also investigated the influence of CeO_2 as the catalyst. As a result, under decreasing settings, the CeO_2 catalyst applied with Ni/Al_2O_3 exhibited the highest activity as the electronic interaction was imparted by the dopant. The methanation activity that incorporated catalyst-doped 1.5 wt% CeO_2 displayed the highest conversion for CO and CO_2, which was 86.34% at 3.674 mol s^{-1}. In fact, inclusion of CeO_2 in $Ni/\gamma\text{-}Al_2O_3$ catalysts appeared to weaken the bond of alumina with nickel, thus increasing the dispersion of nickel on the surface of the catalyst during the catalytic testing. This exemplified that the addition of CeO_2 did not only reduce the deposition of carbon but also managed to accelerate the reaction between steam and the adsorbed species upon the surface of the nickel (Wang and Lu 1998).

In another report, Rynkowski et al. (2000) examined the catalysts in CO_2 methanation, whereby conversion of CO_2 appeared to be maximised for $Ru/CeO_2/Al_2O_3$ and Ru/Al_2O_3 catalysts at 76% and 72%, respectively. In fact, when the temperature exceeded 200 °C, the active catalysts displayed higher stability and higher selectivity towards methane, especially after 340 h. At temperatures that ranged between 200 and 227 °C, selectivity towards methane was near 100%. As such, high temperatures seemed to have a positive impact in reducing catalytic performance, mainly due to the existence of ceria within the catalyst. This also supported by Rosid et al. (2019a) who studied the effect loading of cerium-based catalytic methanation reaction at a calcination temperature of 1000 °C. The results showed that when the Ce content was increased to 60%, the conversion of CO_2 was also increased to 100% at 400 °C reaction temperature; however, a further increase of Ce content up to 85% caused the catalytic performance to decline.

The catalytic activity exhibited by $\alpha\text{-}Al_2O_3\text{-}ZrO_2\text{-}TiO_2\text{-}CeO_2$ composite oxide, along with the support of Ni-based catalyst, was examined with the composite ratio $Al_2O_3/ZrO_2/TiO_2/CeO_2$ (55:15:15:15), respectively. The best catalytic activity was achieved at 300 °C with 81.4% conversion of CO_2 to CH_4 which might be due to improvement in the reducibility nature of the catalysts by the addition of ceria (Abate et al. 2016). The use of ratio-based loadings also has been employed in methanation reaction which gave 100% CO_2 conversion and 80% CH_4 formation at 400 °C reaction temperature. The results showed that the trimetallic oxide catalyst Ru/Mn/Ce (5:35:60)/Al_2O_3 would convert 92.92% of CO_2 gas at 400 °C calcination temperature. Upon increment of the calcination temperature to 700 °C, the catalytic performance reached the maximum 100% CO_2 conversion (Rosid et al. 2015a). Catalytic activity by various ratio-based loadings also has been investigated, and it showed that the performance decreased as the amount of ceria-based catalyst increased which might be due to a blockage of active site by an excess amount of metal oxide (Vicente et al. 2004).

Revisiting the work of Sharma et al. (2016), Ru-substituted CeO_2 catalyst was prepared using a solution combustion method. The findings showed that at 270 °C, the peak of methane appeared, and when it reached the maximum

temperature at 450 °C, the highest methane yield with 55% CO_2 conversion and 99% selectivity for methane was obtained. Meanwhile, the CO_2 conversion was also higher on Mn/Ce-75/Al_2O_3 as compared to Ni/Ce-75/Al_2O_3, Cu/Ce-75/Al_2O_3 and Ce-100/Al_2O_3 over the whole range of studied temperatures. The maximum CO_2 conversion achieved was 69.44% with 27.35% of methane at 300 °C (Toemen et al. 2014).

The $Ce_{0.72}Zr_{0.28}O_2$ was used as a support to the research study by Ocampo et al. (2009), which was prepared with 5 wt% nickel-based catalyst via a pseudo-sol-gel technique. The catalyst revealed higher catalytic activity with 71.5% CO_2 conversion by 98.5% CH_4 selectivity at 350 °C. The operating condition used was 1 atm pressure and a $CO_2/H_2/N_2$ ratio of 36:9:10 with a total gas flow of 55 mL min^{-1}. However, the catalyst started to deactivate after 150 h on stream with 41.1% CO_2 conversion by 94.7% CH_4 selectivity.

The influence of Ce-Zr ratio was further investigated by Ocampo et al. (2011). The catalytic activity of 5Ni/Ce-Zr catalysts with a cerium content of 20 wt%, 60 wt% and 80 wt% was studied at a reaction temperature of 350 °C. The CO_2 conversion for 5Ni/(80:20), 5Ni/(20:80) and 5Ni/(60:40) reached 71.5%, 73% and 79.7% with 98.5%, 99% and 99.3% selectivity to CH_4, respectively. The higher conversion obtained was due to incorporation of Ni^{2+} cations into the Ce-Zr structure. Below than 150 °C, no conversion was detected until 200 °C with lower CO_2 conversion (0.6%). The dosage of catalyst was 150 mg with fixed GHSV at 43,000 h^{-1}.

Recently, Aldana et al. (2013) investigated the catalytic activity of 5Ni/Ce-Zr catalyst at different preparation methods which were pseudo-sol-gel method and wet impregnation method. The CO_2 conversion was higher on 5Ni/Ce-$Zr_{sol\text{-}gel}$ than on 5Ni/Ce-Zr_{imp} over the whole range of studied temperature. At a reaction temperature of 350 °C, the 5Ni/Ce-$Zr_{sol\text{-}gel}$ catalyst showed 79.7% conversion with 99.3% selectivity towards methane while 59.8% conversion with 97.3% methane selectivity over the 5Ni/Ce-Zr_{imp} catalyst. They found that the species on impregnated catalyst was more difficult to be reduced due to the stronger interaction between Ni and support material (Ce-Zr). However, the performance of 5Ni/Ce-Zr_{imp} catalyst was better than that of the Ni/SiO_{2imp} catalyst with 35% CO_2 conversion and 88.3% selectivity towards CH_4. This showed that ceria-zirconia was a better support for Ni compared to silica in the methanation reaction.

In addition, mixed oxide of $Zr_xCe_{30-x}Al_{70}O_\partial$ has also been studied as the supported material for Ni catalyst in autothermal reforming of methane to hydrogen (Puduki and Yaakob 2014). Ni/$Zr_xCe_{30-x}Al_{70}O_\partial$ catalyst showed the highest activity at 650 °C with 75% conversion. Metallic catalyst supported with cerium was remarkable due to its properties which can affect the mechanical and thermal resistance of support, catalytic performance, carbon reduction and metallic dispersion on the catalyst surface (Luisetto et al. 2012). The influence of CeO_2 as a promoter on CO_2 methanation activity and CH_4 selectivity was also studied by Tada et al. (2012). At 300 °C reaction temperature, ceria-supported Ni catalyst exhibited high CO_2 conversion of 90% with 100% CH_4 selectivity compared to Ni/Al_2O_3 catalyst which only gave 20% conversion with 90% selectivity towards methane. This was due to the basic oxide character of CeO_2 support which can adsorb a sufficient amount of CO_2 and reduced it on CeO_2 support owing to its oxygen vacancies. The testing was conducted under a GHSV of 10,000 h^{-1} with the ratio of CO_2:H_2 = 1:4.

Similar observation was found by Ramaroson et al. (1992) over Ni/CeO_2 and Ni/SiO_2 catalysts. At 260 °C reaction temperature with the H_2:CO ratio of 3:1, the Ni/CeO_2 catalyst achieved 11.6% CO conversion and 30.5% selectivity towards methane gas compared to the Ni/SiO_2 catalyst which managed to convert CO with only 2% and 96.4% CH_4 selectivity. Therefore, the use of ceria as a support catalyst gave better result in CO conversion than SiO_2-supported catalyst. The reason was due to the presence of oxygen vacancies on these catalysts which released free electrons and easily ionise. A reversible migration of electrons in the nickel metal can occur, leading to an ease of CO dissociation over the Ni/CeO_2 catalyst.

On the other hand, samarium oxide also has a potential use as a dopant in the methanation process (Chunhui et al. 2010). The addition of Sm to Ba-Ru-K/activated carbon (AC) significantly improved the activity and stability of catalyst. This showed that samarium has enhanced the adsorption of hydrogen on the catalyst surface which leads to higher catalytic performance. Another research has also been conducted on amorphous Ni-Zr-Sm catalysts for CO_2 methanation (Michiaki et al. 1999). This catalyst showed an excellent catalytic activity compared to Ni-Zr catalyst due to the increase number of active nickel sites and stabilisation of tetragonal zirconia by the addition of samarium. This reason has led to the enhancement of catalytic activity. As for zirconia, samarium oxide is regarded as a good support for nickel oxide catalyst in CO_2 methanation.

The performance of samarium as a based catalyst in methanation reaction also has been done by Rosid et al. (2013). The potential catalyst Ru/Mn/Sm (5:35:60)/Al_2O_3 which calcined at 1000 °C gave more than 95% CO_2 conversion with 93.46% CH_4 formation at 300 °C reaction temperature. This showed that samarium has enhanced the performance of catalyst by increasing the rate adsorption of hydrogen onto the surface of catalyst as has been discussed by Michiaki et al. (1999).

Other than that, praseodymium and neodymium also have been studied as based catalysts in the methanation reaction (Rosid et al. 2015c, 2019b). Both catalysts gave > 96% CO_2 conversion at 400 °C reaction temperature with Ru/Mn/Nd (5:20:75)/Al_2O_3 calcined at 1000 °C and Ru/Mn/Pr (5:30:65)/Al_2O_3 calcined at 800 °C. The methane formation

for Ru/Mn/Nd (5:20:75)/Al_2O_3 and Ru/Mn/Pr (5:30:65)/Al_2O_3 catalysts was 40% and 41%, respectively. There are no other reports regarding praseodymium and neodymium as a catalyst in methanation reaction have been found recently.

Physicochemical properties of lanthanide oxide catalysts through characterisation analyses

Physicochemical properties of catalyst are another critical part in the methanation reaction. Different metal oxides demonstrated different structural, active species, morphology, textural particle size, pore distribution and desorption of acidity and basicity of catalysts in order to achieve higher catalytic performance.

The presence of smaller CeO_2 and RuO_2 species with the size range of 78.2 nm to 127 nm successfully improved the catalytic activity of CO_2/H_2 methanation with 100% CO_2 conversion and 80% CH_4 formation (Rosid et al. 2015a). Temperature-programmed reduction (TPR) profile showed the amount of H_2 consumed increased with ceria catalyst which suppressed the metal-support interaction, thus increasing the reducibility of RuO_2 on the catalyst surface at lower temperature as shown in Fig. 1 (Rosid et al. 2018).

Razzaq et al. (2013) also found that the CO_2 desorption peak of Al_2O_3-CeO_2-supported catalyst was dominant at low temperature which was below 100 °C compared to the Al_2O_3-ZrO_2. This region was ascribed to weak basicity related with the weakly adsorbed CO_2 on the catalyst surface. More formation of active sites (CeO_2) observed through XPS analysis led to higher catalytic activity due to transfer of oxygen vacancies from bulk to surface. The formation of oxygen vacancies under reduced Ce^{4+}/Ce^{3+} valance ratio also restrained the coke formation.

The reducibility of Ni/Al_2O_3 catalyst also increased when doped with CeO_2 as well as lowered the reaction temperature

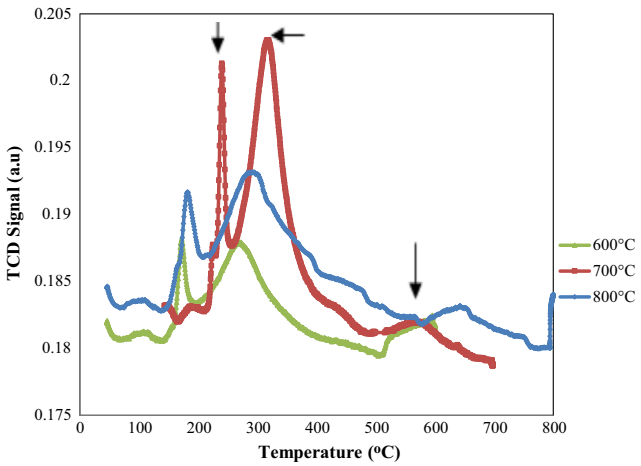

Fig. 1 TPR profile of the Ru/Mn/Ce (5:35:60)/Al_2O_3 catalyst at various calcination temperatures (Rosid et al. 2018)

(Xavier et al. 1999). The oxygen atom (strong base) from the chemisorbed CO molecule created a strong interaction with the Ce^{3+} site Lewis acid. This interaction was weakening the C–O bond and easily hydrogenated to form methane. Jinghuan et al. (2011) reported that incorporation of 5% cerium in cerium-substituted cobalt chromite catalyst deforms the spinel structure and consequently increases the crystal defect by redistribution of metal ion with different oxidation states, thus performing 90% of CH_4 conversion at 465 °C.

Inclusion of ceria investigated by Toemen et al. (2016) appeared to enlarge the surface area and exemplified the presence of mesopores that optimised the size of the pores to promote reactant gas adsorption. Additionally, this particular catalyst showcased type IV that reflected pores in slit shape, along with shapes and size that seemed to be non-uniform. This notion was supported with the HRTEM that showed mixtures of shapes that resembled platelets and rods, in which ceria could have been represented by the platelet shape. On top of that, the HRTEM illustrated the presence of lattice fringes in multiple directions, hence signifying the presence of more than a compound on the surface of the catalyst. The outcome showed that the 0.321 lattice did fit rather well with the related CeO_2 phase.

XRD results expressed that highly spread La_2O_3 during reaction encourages the scattering of NiO on SiC support which enhanced the catalytic activity besides constraining the production of Ni particles (Zhi et al. 2011). TPR results recommended that La_2O_3 could improve the metal-support interaction, hence inhibited the production and agglomeration of metallic particles during the reduction and reaction processes. The XPS result suggested that La_2O_3 in Ni-La/SiC catalyst would increase the adsorption and dissociation of CO_2 molecule by donation of *d*-electron from nickel atoms to vacant anti-bonding π^* orbit of CO_2 molecules. TEM results showed that La_2O_3 encourages the scattering of NiO on the support surface and also can prevent the aggregation and migration of Ni particles as shown in Fig. 2.

As reported by Gao et al. (2009), the $LaNiO_3$ perovskite catalysts activated at 400–700 °C shows a CH_4 selectivity of 98.7–99.2% due to the formation of dispersed small metallic Ni particles which were liable for the high catalytic performance and stability even at high temperature (400–500 °C). H_2-TPD-MS profiles of $La_2O_2CO_3$ under citrate method recommended that hexagonal formation ($La_2O_2CO_3$) also supports the methanation reaction.

The influence of catalytic activation condition by the addition of lanthanum oxide on γ-alumina-supported Co catalyst was also investigated (Kok et al. 2011; Schaper et al. 1985; Rosid et al. 2015b). The presence of this metal oxide has shifted the reduction peak of Co_3O_4 to CoO to a slightly lower temperature around 200 °C which can be beneficial for CO_2 conversion of the catalyst. The pore size distribution was designated to mesoporous structure with an increase in surface

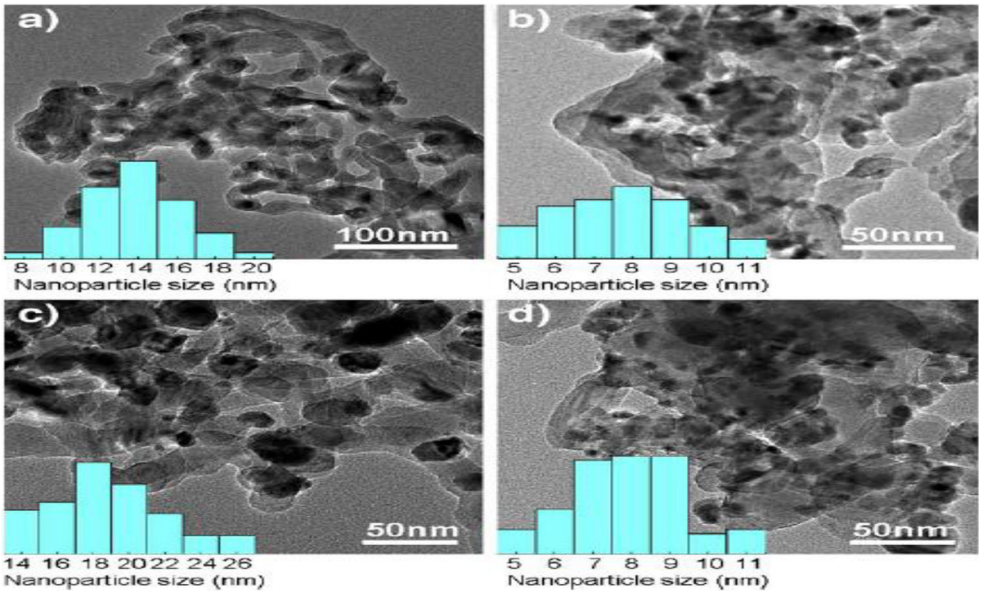

Fig. 2 TEM images of fresh **a** Ni/SiC and **b** Ni-La/SiC and used **c** Ni/SiC and **d** Ni-La/SiC catalysts. Adopted from Zhi et al. (2011)

area with the addition of lanthanum. Similar investigation was conducted by Rosid et al. (2015b) on cobalt-lanthanum-based catalyst supported on Al_2O_3. As shown in Fig. 3, the catalyst displayed amorphous phase which was suppressed by the presence of lanthanum oxide. The low degree of crystallinity was attributed to the larger surface area of catalyst and enhanced the performance of catalyst.

Nickel-based catalysts doped with transition elements such as Mg, Zr, Mo, Mn, Fe, Co and Cu were favourably prepared via sol-gel method (Buang et al. 2008). Pr was selected as a co-dopant among rare-earth metals for all catalysts as it was the most active oxide that has various stable oxidation states (Buang et al. 2008; Holden and Coplen 2004). Ni/Co/Pr was found to be more potential among all catalysts, as it produced highest CH_4 at 350 °C, almost 100% of CO_2 elimination as XRD analysis showed that Co_3O_4 which was a mixture of cubic CoO and Co_2O_3 was the active site for the higher catalytic activity of Ni/Co/Pr. The larger surface area of 59.86 $m^2\ g^{-1}$ for Ni/Co/Pr and Ni/Co showed 38.50 $m^2\ g^{-1}$, indicating that the addition of Pr would enhance the surface area of the catalyst (Buang et al. 2008). Praseodymium was also investigated, and the stability test of Ru/Mn/Pr (5:30:65)/Al_2O_3 was carried out consistently up to 7 h through 96% CO_2 conversion. The low degree of crystallinity was patterned in XRD due to the praseodymium with small particle size as supported with FESEM analysis. RuO_2 was assigned as an active species in this catalyst and supported by EDX with abundance of Ru mass ratio (Rosid et al. 2015c).

As summary, the study of physicochemical properties of each catalyst is a main point to attain higher catalytic performance. The best physicochemical properties of lanthanide oxide are higher surface area, reduced active species at lower temperature, presence of oxygen vacancies and basic properties to comply with acidity of CO_2 gas.

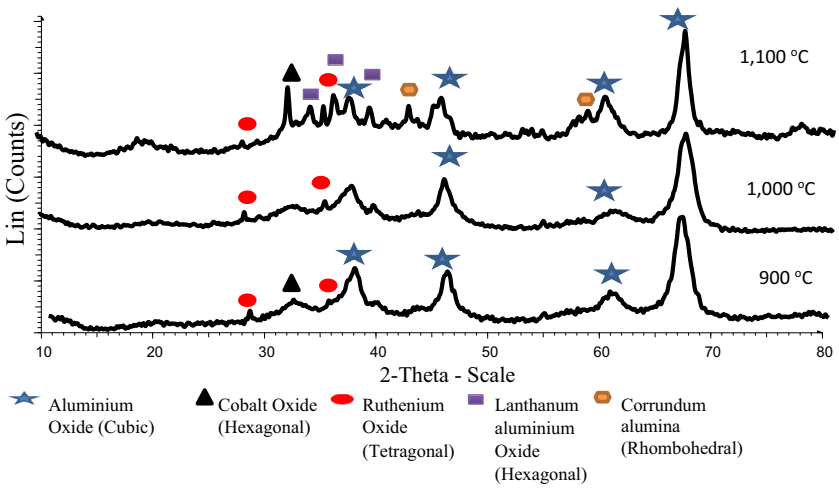

Fig. 3 XRD diffractograms of the Ru/Co/La(5:35:60)/Al_2O_3 catalyst calcined at various temperatures (900 °C. 1000 °C and 1100 °C for 5 h) (Rosid et al. 2015b)

Mechanism of catalytic CO_2 methanation reaction

The mechanism of heterogeneous catalyst commonly follows the Langmuir-Hinshelwood (LH) mechanism in which both reactants are adsorbed on the surface, collide and form products (Eq. (3)). It is composed of various steps on the surface of the catalyst which include the adsorption, surface reaction and desorption of metal species. However, the formation of intermediate from the reaction depends on the nature and mode of adsorption of reactants and surface of reaction on the adsorbed species. In other words, it relies on the reactiveness of metal oxide species towards CO_2 and H_2 molecules. Therefore, insight into the mechanism of chemical reaction is important to optimise the methanation reaction and improves the performance.

$$\begin{gathered} A_{(reactant)} \rightleftharpoons A_{(absorbed)}, B_{(reactant)} \rightleftharpoons B_{(adsorbed)} \\ A_{(absorbed)} + B_{(adsorbed)} \rightleftharpoons C_{(adsorbed)} \\ C_{(adsorbed)} \rightleftharpoons C_{(product)} \end{gathered} \quad (3)$$

Several studies have stated that the mechanism of methanation comprised direct detachment of CO_2 to $CO_{(ads)}$ and $O_{(ads)}$ on the catalyst surface, with $CO_{(ads)}$ being subsequently hydrogenated to CH_4 (Xu et al. 2006; Razzaq et al. 2013; Beuls et al. 2011; Marwood et al. 1997; Kopyscinski et al. 2011; Sehested et al. 2004). At initial, CO_2 and H_2 molecules reacted with the catalyst surface (S) by chemisorption to create an active species that adsorbed onto the catalyst surface (Eqs. (4) and (5)). Both adsorbed species then reacted to each other (Eq. (6)) and, finally, released products of methane and water (Eqs. (7) and (8)).

$$CO_2 + S \rightleftarrows CO_{2(ads)} \quad (4)$$

$$H_2 + S \rightleftarrows H_{2(ads)} \quad (5)$$

$$CO_{2(ads)} + H_{2(ads)} \rightleftarrows CH_{4(ads)} + H_2O_{(ads)} \quad (6)$$

$$CH_{4(ads)} \rightleftarrows CH_{4(desorp)} + S \quad (7)$$

$$H_2O_{(ads)} \rightleftarrows H_2O_{(desorp)} + S \quad (8)$$

where S is the catalyst surface, (ads) is the adsorption of molecule on the catalyst surface and (desorp) is the desorption of molecule on the catalyst surface.

In fact, this particular concept was in line with Solymosi et al. (1981), who asserted the process of adsorption and dissociation of CO_2 with transition metals took place to transfer electrons in order to generate radical species in anion structure. Hence, adsorbed species decreased energy to minimise obstacle in activation between species at gas phase and support adsorption. Next, the H atom species that was active got attached to O atom in order to generate water as its by-product. This process was continuous until all the free carbon atoms were completely attached with H atoms in order to generate CH_4.

Different mechanistic perspectives were found by Miao et al. (2016). The methanation process involved two categories which were associative and dissociative. In the associative scheme, the hydrogenation process took place in the C–O bond-breaking process while the dissociative scheme did not involve hydrogenation for breaking C–O bond. Then, the hydrogen atom was then attracted to free carbide to form methane molecule. Referring to Hu et al. (2012), they claimed that metal-based oxide and dopant played different roles in the hydrogenation reaction. Metal-based oxide initiated the reaction by binding with CO_2 molecule, whereas dopant activated the reaction by providing H atoms that were needed for further hydrogenation.

The finding of Kim et al. (2010) confirmed the mechanism of Pd-MgO/SiO_2 catalyst was started with initiation of MgO binding together with CO_2 molecule to form magnesium carbonate. The Pd was essential to dissociate H_2 molecule and supplied H atoms to carbonates on MgO, for hydrogenation of oxygen species, and produced two molecules of water. A free C on MgO was hydrogenated to CH_4 product. The similar concept of mechanism of CO_2 methanation was also reported by Jacquemin et al. (2010). The first step could be the chemisorption of CO_2 on reduced Rh/γ-Al_2O_3 catalyst followed by the bond breaking of CO_2 to form $CO_{(ads)}$ and $O_{(ads)}$ species. The formation of $CO_{(ads)}$ was supported by the presence of peaks belonging to linear Rh-CO (2048 cm^{-1}), Rh^{3+}-CO (2123 cm^{-1}) and Rh-$(CO)_2$ (2024 cm^{-1} and 2092 cm^{-1}). The adsorbed Rh-$(CO)_2$ was the most reactive species with hydrogen. The $CO_{(ads)}$ was then detached into C and O on the surface, and further hydrogenation of C took place to produce CH_4. No CO_2 conversion was observed over unreduced Rh/γ-Al_2O_3 catalyst compared to 0.63% conversion (99% CH_4 selectivity) of reduced catalyst at room temperature.

The species that adsorbed on the Ru/Mn/Ce-65/Al_2O_3 catalyst surface during reaction was examined by Toemen et al.

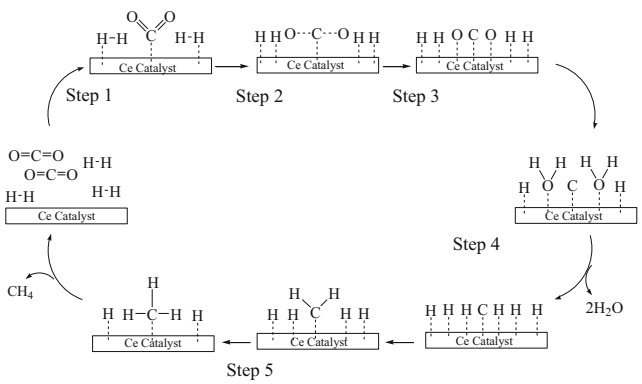

Fig. 4 Proposed mechanism for Ru/Mn/Ce-65/Al_2O_3 catalysts (Toemen et al. 2016)

(2016). The investigated mechanism only portrayed direct adsorption and dissociation for CO_2 and H_2, as illustrated in Fig. 4. Initially, all molecules of H_2 and CO_2 had been directed towards the catalyst surface, wherein the C atom of CO_2 had been coordinated directly to the catalyst of cerium oxide in order to generate inorganic carboxylate, as step 1. Next, in step 2, the surface of the catalyst displayed the coordination of CO_2 molecules that had been adsorbed (step 2). As such, the peak of adsorption noted at 2087 cm^{-1} could be associated to the adsorbed CO that reflected a configuration in linear manner on the Ce catalyst surface (Asedegbega-Nieto et al. 2005; Kramer et al. 2009). After that, the adsorbed H_2 molecules were dissociated, hence turning into H atom species followed by dissociation of CO_2 molecules (step 3). In step 4, as asserted by Kim et al. (2010), hydrogenation of oxygen species occurred in a spontaneous manner, thus releasing dual water molecules. As for the H atoms that were released from O, they formed methane after combining with C molecules.

The mechanism of Ru/Mn/Sr-65/Al_2O_3 was extended using FTIR analysis to identify the surface species present during the reaction process. Figure 5 shows two broad O–H regions at 3434 cm^{-1} and 1635 cm^{-1} which were assigned to the stretching and bending vibration of adsorbed water (Eckle et al. 2011; Karelovic and Ruiz 2013). Meanwhile, adsorption peak at 2071 cm^{-1} corresponded to CO-adsorbed linear or bridged configuration (Stevens et al. 2008) on the Sr catalyst surface. When the temperature was increased to 100 °C, two new peaks around 1769 cm^{-1} and 1462 cm^{-1} were observed which were assigned to carbonyl or carbonate species. The formate species was not detected since no (C-H) peak was observed in FTIR. However, at 200 °C reaction temperature, the carbonate species was further hydrogenated by detachment hydrogen atom to form formate, leading to a decrease in carbonate intensity. The new adsorption peaks were observed at 2962 cm^{-1} and 2851 cm^{-1} which were assigned to CH_3 and CH_2 symmetric, respectively. These peaks were sharp and intense at 200 °C but decreased the intensity at 210 °C due to the release of methane gas. Therefore, higher CH_4 gas was detected at this temperature.

From the FTIR spectra in Fig. 5, the mechanism channel is depicted in Fig. 6 that shows the incorporated CO_2 adsorption, reflecting step 1, which suggested the formation of monodentate carbonate by attaching oxygen to the catalyst surface. Next, in step 2, two formations took place at lower surface of CO_2 coverage, which were bidentate carbonate as well as bridged bidentate carbonate. In step 3, the products of steps 1 and 2, which were hydrogenated carbonate species, were attached to free H atoms to generate formate species (HCOO), apart from releasing a water molecule. This hydrogenation process was continued to generate dioxomethylene (H_2COO) (step 4) and formaldehyde (CH_2O) (step 5) (Sahki et al. 2011), including methoxy species (Aldana et al. 2013) that contained a methyl group attached to oxygen (–OCH_3) (step 6), as well as a water molecule prior to finalising the whole process by producing methane gas.

Overall, there were still arguments on reaction intermediates and methane formation involved in this process (Eckle et al. 2011; Karelovic and Ruiz 2013; Gao et al. 2015). Kudo and Komatsu (1999) presumed that the current methanation mechanism proceeds via formation of formate intermediate. The CO_2 molecule was adsorbed on the surface as a metal carbonate and then reduced by the hydrogen to the surface formate. Then, the formate decomposed to a surface active carbon on the Ru catalyst and was then hydrogenated to form methane gas.

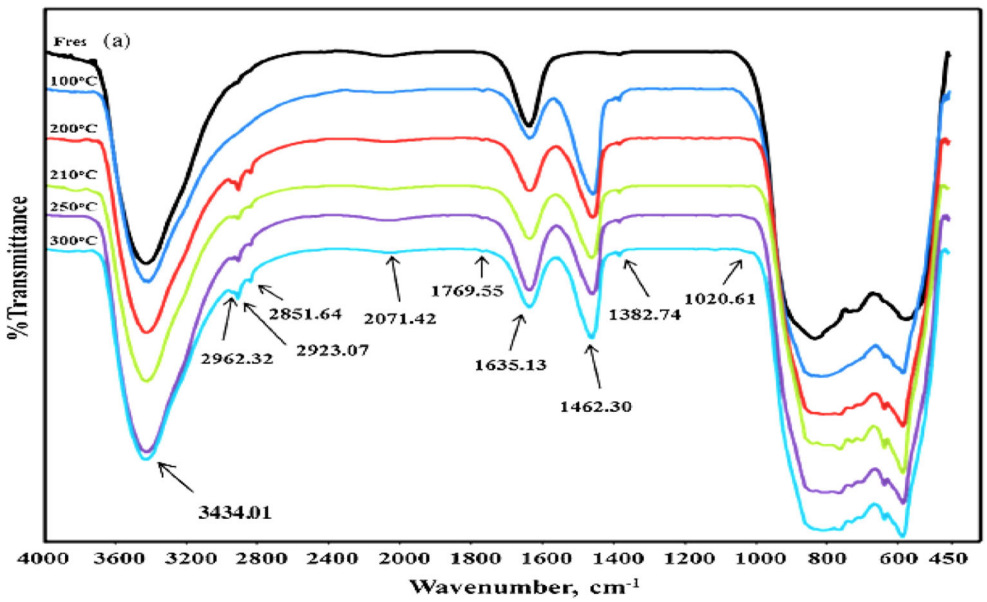

Fig. 5 FTIR spectra for Ru/Mn/Sr-65/Al_2O_3 catalysts (Toemen et al. 2016)

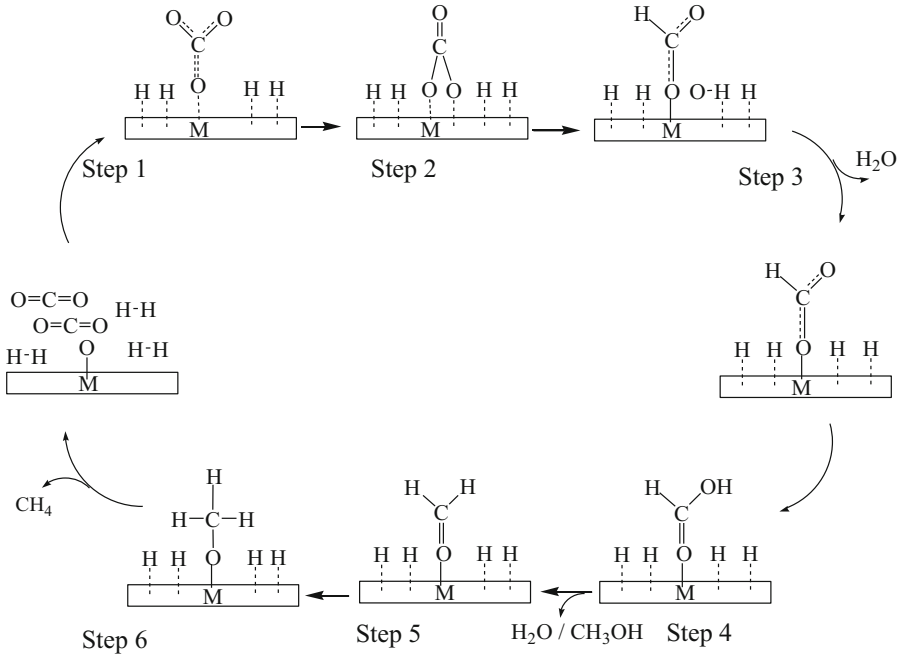

Fig. 6 Proposed mechanism over the Ru/Mn/Sr (5:30:65)/Al_2O_3 catalyst calcined at 1000 °C for 5 h (Toemen et al. 2016). M = Ru/Mn/Sr (5:30:65)/Al_2O_3 catalyst

*M = Ru/Mn/Sr (5:30:65)/Al_2O_3 catalyst

Here, the role of Ru was to activate the dissociation of hydrogen molecule to interact with formate for the methanation process. The formation of intermediate formate species over 2% Ru/TiO_2 catalyst proposed by Marwood et al. (1997) was slightly different from the mechanism of Kudo and Komatsu (1999). The CO_2 was firstly reacted to the hydroxyl group on the catalyst surface to form a surface-bound hydrogen carbonate species, HCO_3^-. It was then reduced with metal-adsorbed hydrogen to an interfacial formate species, $HCOO^-$. The interfacial formate decomposed to adsorb CO species while regenerating the surface hydroxyl group again. Lastly, the hydrogenation of CO adsorbed species with adsorbed hydrogen in order to produce methane gas. The similar mechanism had been observed by Aldana et al. (2013) on Ni-based ceria-zirconia catalysts. They found that H_2 was dissociated on Ni^0 sites while CO_2 was initiated on the ceria-zirconia surface to produce carbonates which could be hydrogenated into formate and further into methoxy species. This mechanism involved weak basic site for adsorption of acidic CO_2 and indicates a stable metal-support interface.

Pan et al. (2014) have proposed that CO_2 preferably attached at the oxygen site adjacent to Ce(III) compared with adjacent to Ce(IV)/Zr or surface hydroxyl site. The adsorption species were revealed during the mechanistic studies which were monodentate carbonate adjacent to Ce(IV), Ce(III) or Zr, bidentate carbonate adjacent to Ce(III) or Ce(IV) and hydrogen carbonates in the surface hydroxyl site. Interestingly, monodentate carbonate on Ce(III) was easier to be hydrogenated than Ce(IV). Hahn et al. (2013) also found that CO_2 was preferably adsorbed in monodentate configuration to form a carbonate species with a surface oxygen atom on CeO_2(III).

Wang et al. (2016) investigated the reaction of CO_2 methanation via formate species in the catalyst of Ru/CeO_2 through in situ DRIFT infrared spectroscopy with steady-state isotope transient kinetic analysis. CO_2 methanation over Ru/Al_2O_3 catalyst underwent CO route due to the absence of oxygen vacancy. Next, the Ce–O bond on the surface of CeO_2 was attacked by dissociated H atoms to generate vacancies at hydroxyl surface, oxygen and Ce^{3+}. Upon usage of CO_2, carbonyl peak shift was absent until the temperature was hiked to 250 °C. It was noteworthy to highlight that the CH_4 peak at 3017 cm^{-1} was noted upon temperature hike, thus signifying 250 °C as the carbonyl activation temperature for Ru/Al_2O_3. Nevertheless, the carbonyl for Ru/CeO_2 appeared at 150 °C, which succeeded in converting to CH_4 exceeding 250 °C. Meanwhile, the activation temperature to convert Ce^{3+} to Ce^{4+} (25 °C) seemed to coincide with that temperature employed to convert CO_2 to CO_2^-. In addition, CO_2^- activation temperature to formate appeared to agree rather well with the initial temperature of 25 °C used to reduce the surface of hydroxyl. This showed that formate was derived from CO_2 hydrogenation and enhanced by the H atom found on the hydroxyl surface that was upon the surface of CeO_2. Simultaneously, methanol bands at 1008 cm^{-1} and 3659 cm^{-1} had been observed during the reaction process involving Ru/CeO_2 catalyst, which further signified the fact that the step to determine the rate referred to formate detachment from methanol. At the final step, methane was easily produced after methanol was hydrogenated.

CO_2 adsorption on the ceria surface over Ni/CeO_2 catalyst also has been suggested to occur through hydrocarbonate and formate intermediates to form methane (Konishcheva et al. 2016). The methanation reaction proceeded through dissociation of hydrogen from Ni particles. The presence of hydrocarbonates and formates on the ceria surface over Ni/CeO_2 indicates the participation of CO_2 derivative species adsorbed on ceria in the reaction. These intermediate species was converted to methane by hydrogenation reaction with hydrogen migrated from Ni surface catalyst. This mechanism was also suggested by Aldana et al. (2013) and Pan et al. (2014) who were using Ni/$Zr_{0.5}Ce_{0.5}O_2$ catalyst.

Sharma et al. (2016) have reported the mechanistic study of CO_2 methanation over Ru-substituted CeO_2 catalyst that has been prepared by combustion. The results showed that CO_2 was adsorbed on the surface of $Ce_{0.95}Ru_{0.05}O_2$ and formed carbonate intermediate in the presence of H_2. During dissociation, carbonates led to adsorption of CO which formed methane upon reaction with H_2. The catalyst produced methane at 270 °C, reading the highest methane yield at 450 °C. Above 450 °C, the concentration of CO and H_2 increased, the concentration of O_2 increased slightly while the concentration of CH_4 decreased. This might be due to unreacted carbonates that decomposed to O_2 and CO above 450 °C. From the results, the peak of formate was not observed by FTIR analysis, which suggested that the reaction pathway was only via formation of carbonate and CO intermediates.

The interesting side product that may be produced from the reaction is methanol (CH_3OH), but the production should be conducted in the presence of pressure. Borodko and Somorjai (1999) who studied on the CuO/ZnO/Al_2O_3 catalyst found that CO_2 conversion and CH_3OH selectivity increased with an increase in the pressure. The CO_2 conversion was increased from 3.1 to 11.9% as well as the methanol selectivity from 5.3 to 47.1% when the pressure was incremented from 1 to 75 bar at the flow rate 2 L h^{-1} and 230 °C. Meanwhile, the ethanol selectivity was strongly enhanced by changes with basic additives such as alkali and alkaline earth metals (Matsuzaki et al. 1997; Chang et al. 2017).

The mechanism of CO_2 on Ni(111) lattice surface catalyst was also confirmed by computational modelling (Choe et al. 2005). The elementary reaction steps consisted of two mechanisms which were carbon formation and carbon methanation. The activation energy of dissociation of CO_2 to form CO intermediate and atomic oxygen was valued at 1.27 eV. The detachment of CO into C and O (step 2) was considered as rate determining based on calculated activation energy of 2.97 eV, the highest from all the elementary steps. Finally, the hydrogenation of C occurred on the surface catalyst until methane gas is produced.

From these mechanisms, it showed that there were many side products that will be produced from the CO_2 methanation reaction, particularly CO gas intermediate species. All possible variables such as different metals, supports, reaction conditions and preparation methods can lead to different mechanisms and yields of products.

Conclusion and future aspect

Fossil fuels are the most demanding world's energy supply with almost more than 98% of needs in daily activity. Unfortunately, the by-product from combustion of fossil fuels has led to emission of CO_2 to the atmosphere which is one of the major sources of GHGs, especially from transportation (Sudhanshu et al. 2011). Several methods have been approached in order to reduce the production of CO_2 gas and prevent the global warming from becoming worst (Niven 2005; Rahman et al. 2017). Accordingly, the raw natural gas contains impurities of CO_2 gas which contributed to the annual increment in the percentage of CO_2 gases in Malaysia and globally. Therefore, methanation reaction has been chosen as one of the potential technologies to convert waste (CO_2) gas to wealth (CH_4) gas in the combustion of natural gas in order to reduce emission of CO_2 to atmosphere. A few parameters have been studied which were preparation methods, support of catalysts and promoter utilising rare-earth metal oxide which gave an excellent performance. A mechanistic study also has been investigated by many researchers to determine the pathway that contributes more methane product and minimises the production of by-products. In summary, a future aspect of research should be specified on optimisation of catalyst parameter in order to achieve excellent CO_2 conversion and CH_4 formation at low reaction temperature and possess long-term stability. Alternatively, response surface methodology should be useful in the methanation reaction for the optimisation of critical parameters such as calcination temperature, ratio-based loading, catalyst dosage, time of reaction, temperature for reduction condition and so on. This method has great advantage towards research in terms of time saving since only a few experimental points needed for its application (Khuri and Mukhopadhyay 2010). The application of Box-Behnken design in industrial research is widespread due to its economical design and improvement in response to chemical and processing fields (Myers et al. 1992). Other than that, a modelling study also should be conducted in order to support the actual reaction that occurs in methanation reaction. This modelling study also can give an exact kinetic energy of active species which lead to higher catalytic performance.

Acknowledgements The authors thank the Universiti Sultan Zainal Abidin, Universiti Teknologi Malaysia (GUP 13H34) and the Ministry of Higher Education (MOHE) for FRGS vote no. 5F076.

References

Aasberg-Petersen K, Dybkjaer I, Ovesen CV, Schjodt NC, Sehested J, Thomsen SG (2011) Natural gas to synthesis gas-catalysts and catalytic process. J Nat Gas Sci Eng 3:423–459

Abate S, Mebrahtu C, Giglio E, Deorsola F, Bensaid S, Perathoner S, Pirone R, Centi G (2016) Catalytic performance of γ-Al_2O_3-ZrO_2-TiO_2-CeO_2 composite oxide supported Ni-based catalysts for CO_2 methanation. Ind Eng Chem Res 55:4451–4460

Abdulrahman RK, Sebastine I (2012) Natural gas sweetening by using iron sponge process: a case study of Hamilton North Gas Field. Am J Sci Res 71:135–142

Abe T, Tanizawa M, Watanabe K, Taguchi A (2009) CO_2 methanation property of Ru nanoparticle-loaded TiO_2 prepared by a polygonal barrel-sputtering method. Energy Environ Sci 2:315–321

Bakar WAWA, Ali R, Toemen S (2012) Catalytic methanation reaction over supported nickel–ruthenium oxide base for purification of simulated natural gas. Scientia Iranica 19(3):525–534

Akin AN, Ataman M, Aksoylu AE, Önsan ZI (2002) CO_2 fixation by hydrogenation over coprecipitated Co/Al_2O_3. React Kinet Catal Lett 76(2):265–270

Aldana PAU, Ocampo F, Kobl K, Louis B, Thiboalt-Starzyk F, Daturi M, Bazrin P, Thomas S, Roger AC (2013) Catalytic CO_2 valorization into CH_4 on Ni-based ceria-zirconia. Reaction mechanism by operando IR spectroscopy. Catal Today 215:201–207

Aleman-Nava GS, Casiano-Flores VH, Cardenas-Chavez DL, Charez RD, Scarlat N, Mahlknecht J, Dailemand J-F, Parra R (2014) Renewable energy research progress in Mexico: a review. Renew Sust Energ Rev 32:140–153

Anerousis JP, Whitman SK (1984) An updated examination of gas sweetening by the iron sponge process. 1984. Society of Petroleum Engineers of AIME, 59th Annual Technical Conference and Exhibition held in Houston, Texas. Sept 16–19. 1–12

Arsalanfar M, Mirzaei AA, Bozorgzadeh HR, Atashi H, Shahriari S, Pourdolat A (2012) Structural characteristics of supported cobalt–cerium oxide catalysts used in Fischer–Tropsch synthesis. J Nat Gas Sci Eng 9:119–129

Asedegbega-Nieto E, Guerrero-Ruíz A, Rodríguez-Ramos I (2005) Study of CO chemisorption on graphite-supported Ru–Cu and Ni–Cu bimetallic catalysts. Thermochim Acta 434(1–2):113–118

Bakar WAWA, Ali R, Kadir AAA, Rosid SJM, Mohammad NS (2012) Catalytic methanation reaction over alumina supported cobalt oxide doped noble metal oxides for the purification of simulated natural gas. J Fuel Chem Technol 40(7):822–830

Beuls A, Swalus C, Jacqiemin M, Heyen G, Kavelovic A, Ruiz P (2011) Methanation of CO_2: further insight into the methanation over Rh/Al_2O_3 catalyst. Appl Catal B Environ 113–114:2–10

Beuls A, Swalus C, Jacquemin M, Heyen G, Kareloviz A, Ruiz P (2012) Methanation of CO_2: further insight into the mechanism over Rh/γ-Al_2O_3 catalyst. Appl Catal B Environ 113–114:2–10

Biernat K, Gisw SBI (2012) Review of technology for cleaning biogas to natural gas quality. Combust Engines 1:33–39

Boaro M, Colussi S, Trovarelli A (2019) Ceria-based materials in hydrogenation and reforming reactions for CO_2 valorization. Front Chem. In press. https://doi.org/10.3389/fchem.2019.00028

Borodko Y, Somorjai GA (1999) Catalytic hydrogenation of carbon oxides—a 10-year perspective. Appl Catal A Gen 186(1–2):355–362

Brooks KP, Hu J, Zhu H, Kee RJ (2007) Methanation of carbon dioxide by hydrogen reduction using the Sebastier process in microchannel reactors. Chem Eng Sci 62(4):1161–1170

Buang NA, Wan Abu Bakar WA, Marsin FA, Razali MH (2008) CO_2/H_2 methanation on nickel oxide based catalysts doped with various elements for the purification of natural gas. Malaysian J Anal Sci 12(1):217–223

Centi G, Quadrelli EA, Perathoner S (2013) Catalysis for CO_2 conversion: a key technology for rapid introduction of renewable energy in the value chain of chemical industries. Energy Environ Sci 6:1711–1731

Chang WR, Hwang JJ, Wu W (2017) Environmental impact and sustainability study on biofuels for transportation application. Renew Sust Energ Rev 67:277–288

Chen X, Zhou H, Chen S, Dong X, Lin W (2007) Selective oxidation of CO in excess H_2 over Ru/Al_2O_3 catalyst modified with metal oxide. J Nat Gas Chem 16:409–414

Choe S, Kang H, Kim S, Park S, Park D, Huh D (2005) Adsorbed carbon formation and carbon hydrogenation for CO_2 methanation on the Ni(111) surface: ASED-MO study. Bull Kor Chem Soc 26:1682–1688

Chunhui Z, Yifeng Z, Huazhang L (2010) Effect of samarium on methanation resistance of activated carbon supported ruthenium catalyst for ammonia synthesis. J Rare Earths 28:552–555

Curry RN (1981) Fundamental of natural gas conditioning. Penwell Books Publishing Company, Oklahoma, pp 66–67

Djinovic P, Galletti C, Specchia S, Specchia V (2011) Ru based catalysts for CO selective methanation reaction in H_2-rich gasses. Catal Today 164(1):282–287

Dong X, Pi G, Ma Z, Dong C (2017) The perform of the natural gas industry in the PR of China. Renew Sust Energ Rev 73:582–593

Dorner RW, Willaver HD, Hardy DR (2014) United States Patent 8658554 B2. Retrieved on February 25, 2014 from http://www.freepatentsonline.com/

Duisberg M, Maier WF, Kraemer M. (2008) WO2008110331A/ Retrieved on 18 Sept 2008. http://www.freepatentsonline.com/

Duissberg M, Frankfurt, Maier WF, Kraemer M (2010a) United State Patent 20100168257 A1. Retrieved on July 1, 2010 from http://www.freepatentsonline.com/

Duissberg M, Maier WF, Kraemer M (2010b) Patentscope W02008/110331 A1. Retrieved on September 18, 2008 from http://www.freepatentsonline.com/

Eckle S, Antang HG, Behm RJ (2011) Reaction intermediates and side products in the methanation of CO and CO_2 over supported Ru catalysts. J Phys Chem C 115:1361–1367

Ertesva IS, Kvamsdal HM, Bolland O (2005) Energy analysis of gas turbine combined-cycle power plant with pre-combustion CO_2 capture. Energy 30:5–39

Feng YY, Yang W, Chen S, Chu W (2014) Cerium promoted nano nickel catalysts Ni-Ce/CNTs and Ni/Ce/Al_2O_3 for CO_2 methanation. Integr Ferroelectr 151:116–125

Finch JN (1979) United States Patent 4168276. Retrieved on September 18, 1979 from http://patft.uspto.gov/

Finch JN, Ripley DL (1976) United States Patent 3988334. Retrieved on October 26, 1976 from http://www.freepatentsonline.com/

Fred S (2008) Integrated gasification combined cycle for carbon capture and storage. Gulf Professional Publishing, Burlington

Frohning D, Horn G (1983) United States Patent 4368142. Retrieved on January 11, 1983 from http://www.freepatentsonline.com/

Gao J, Jia LS, Fanf WP, Li QB, Song H (2009) Methanation of carbon dioxide over the $LaNiO_3$ perovskite catalysts activated under the reactant stream. J Fuel Chem Technol 37(5):573–577

Gao J, Liu Q, Gu F, Liu B, Zhong Z, Su F (2015) Recent advances in methanation catalysts for the production of synthetic natural gas. RSC Adv 5:22759

Habazaki H, Yamasaki M, Zhang B, Kawashima A, Kohno S, Takai T, Hashimoto K (1998) Co-methanation of carbon monoxide and carbon dioxide on supported nickel and cobalt catalysts prepared from amorphous alloy. Appl Catal A Gen 172:131–140

Hahn KR, Iannuzzi M, Seitsonen AP, Hutter J (2013) Coverage effect of the CO_2 adsorption mechanisms on CeO_2 (111) by first principle analysis. J Phys Chem C 117:–1701

Haldor Topsøe A/S (2005) Methanation of CO over nickel mechanism and kinetics at high H_2/Co ratios. J Phys Chem B 109(6):2432–2438

Happel J, Hnatow MA (1979) United State Patent 4260553 A. Retrieved on March 5, 1979 from http://patft.uspto.gov/

Henville KE (2000) Patentscope W000/16901. Retrieved on July 1, 2010 from http://www.freepatentsonline.com/

Hoekman SK, Broch A, Robbins C, Purcell R (2010) CO_2 recycling by reaction with renewably-generated hydrogen. Int J Greenhouse Gas Control 4(1):44–50

Holden N, Coplen T (2004) The periodic table of the elements: Chemistry International 26(1):8–9

Hu D, Gao J, Ping Y, Jia L, Gunawan P, Zhong Z, Xu G, Gu F, Su F (2012) Enhanced investigation of CO methanation over Ni/Al_2O_3 catalysts for synthetic natural gas production. Ind Eng Chem Res 51: 4875–4886

Jacquemin M, Beuls A, Ruiz P (2010) Catalytic production of methane from CO_2 and H_2 at low temperature: insight on the reaction mechanism. Catal Today 157(1–4):462–466

Jenewein B, Fuchs M, Hayek K (2003) The CO methanation on Rh/CeO_2 and CeO_2/Rh model catalysts: a comparative study. Surf Sci 532–535:364–369

Jinghuan C, Wenbo S, Junhua L (2011) Catalytic combustion of methane over cerium-doped cobalt chromite catalysts. Catal Today 175(1): 216–222

Kakaee A-H, Paykani A, Ghajar M (2014) The influence of fuel composition on the combustion and emission characteristics of natural gas fueled engines. Renew Sust Energ Rev 38:64–78

Karelovic A, Ruiz P (2013) Mechanistic study of low temperature CO_2 methanation over Rh/TiO_2 catalysts. J Catal 301:141–153

Khan MA (2015) Modelling and Forecasting the demand for natural gas in Pakistan. Renew Sust Energ Rev 49:1145–1159

Khuri AI, Mukhopadhyay S (2010) Response surface methodology. Wiley Interdiscip Rev: Comput Stat 2(2):128–149

Kim HY, Lee HM, Park JN (2010) Bifunctional mechanism of CO_2 methanation on Pd-MgO/SiO_2 catalyst: independent roles of MgO and Pd on CO_2 methanation. J Phys Chem C 114(15):7128–7131

Kobylinski TP, Swift HE (1976) United States Patent 3947483. Retrieved on March 30, 1976 from http://www.freepatentsonline.com/

Kok E, Scott J, Cant N, Trimm D (2011) The impact of ruthenium, lanthanum and activation conditions on the methanation activity of alumina supported cobalt catalysts. Catal Today 164(1):297–301

Konishcheva MV, Potemkin DI, Badmaev SD, Snytnikov PV, Paukshtis EA, Sobyanin VA, Parmon VN (2016) On the mechanism of CO and CO_2 methanation over Ni/CeO_2 catalysts. Top Catal 59:1424–1430

Kopyscinski J, Schildhaver TJ, Biollaz SMA (2011) Methanation in a fluided bed reactor with high initial CO partial pressure: part 1. Experimental investigation of hydrodynamics, mass transfer effects and carbon deposition. Chem Eng Sci 66(5):924–934

Kramer M, Stowe K, Duisberg M, Muller F, Reiser M, Sticher S, Maier WF (2009) The impact of dopants on the activity and selectivity of a Ni-based methanation catalyst. Appl Catal A Gen 369:42–52

Kudo K, Komatsu K (1999) Selective formation of methane in reduction of CO_2 with water by Raney alloy catalyst. J Mol Catal A Chem 145:257–264

Lee HC, Kim S, Lee KH, Lee OH, Park ED, Ko EY (2006) United State Patent 8067332 B2. Retrieved on May 3, 2006 from http://www.freepatentsonline.com/

Li Y (2014) United State Patent 8629077 B2. Retrieved on Jan 14, 2014 from http://www.freepatentsonline.com/

Liu H, Zou X, Wang X, Lu X, Ding W (2012a) Effect of CeO_2 addition on Ni/Al_2O_3 catalysts for methanation of carbon dioxide with hydrogen. J Nat Gas Chem 21(7):703

Liu Z, Chu B, Zhai X, Jin Y, Cheng Y (2012b) Total methanation of syngas to synthetic natural gas over Ni catalyst in a micro-channel reactor. Fuel 95:599–605

Luisetto I, Tuti S, Bartolomeo ED (2012) Co, Ni supported on CeO_2 as selective bimetallic catalyst for dry reforming of methane. Int J Hydrog Energy 57:15992–15999

Marwood M, Doepper R, Renken A (1997) In-situ surface and gas phase analysis for kinetic studies under transient conditions: the catalytic hydrogenation of CO_2. Appl Catal A Gen 151:223–246

Matsuzaki T, Hanaoka T, Takeuchi K, Arakawa H, Sugi Y, Wei K, Dong T, Reinikainen M (1997) Oxygenates from syngas over highly dispersed cobalt catalysts. Catal Today 36(3):311–324

Miao B, Ma SSK, Wang X, Su H, Chan SH (2016) Catalysis mechanisms of CO_2 and CO methanation. Catal Sci Technol 6:4048–4058

Michael K, Golab A, Shulakova V, Ennis-Kinga J, Allinson G, Sharma S, Aiken T (2010) Geological storage of CO_2 in saline aquifers—a review of the experience from existing storage of operation. Int J Greenh Gas Control 4:659–667

Michiaki Y, Mtsuru K, Eiji A Hiroki H, Asahi K, Katsuhiko A, Koji H (1999) CO_2 methanation catalysts prepared from amorphous Ni-Zr-Sm and Ni-Zr-misch metal alloy precursors. Journal Material Science & Engineering. Institute for Materials Research, Tohoku University, Sendai, Japan

Mokhatab S, Poe WA, Speight JG (2006) Handbook of natural gas: transmission and processing. Elsevier, Amsterdam

Munik P, Velthoen MEZ, Jongh PED, Jong KPD, Gommes CJ (2014) Nanoparticle growth in supported nickel catalysts during methanation reaction—larger is better. Angew Chem Int Ed 53:9493–9497

Myers RH, Khuri AI, Vining G (1992) Response surface alternative to the Taguchi robust parameter design approach. Am Stat 46(2):131–139

Niven RK (2005) Ethanol in gasoline: environmental impacts and sustainability review article. Renew Sust Energ Rev 9(6):535–555

Ocampo F, Louis B, Roger AC (2009) Methanation of carbon dioxide over nickel-based $Ce_{0.72}Zr_{0.28}O_2$ mixed oxide catalysts prepared by sol-gel method. Appl Catal A Gen 369:90–96

Ocampo F, Louis B, Kiwi-Minsker L, Roger A-C (2011) Effect of Ce/Zr composition and noble metal promotion on nickel based $Ce_xZr_{1-x}O_2$ catalysts for carbon dioxide methanation. Appl Catal A Gen 392(1–2):36–44

Ortego JD, Jothimurugesan JK, Espinoza RL, Coy KL, Ortego CB (2006) United State Patent 7071239 B2. Retrieved on July 4, 2006 from http://www.freepatentsonline.com/

Pan Q, Peng J, Sun T, Gao D, Wang S, Wang S (2014) CO_2 methanation on Ni/$Ce_{0.5}Zr_{0.5}O_2$ catalysts for the production of synthetic natural gas. Fuel Process Technol 123:166–171

Pargeter JK, Ahmad UMU (1980) United States Patent 4196100. Retrieved on April 1, 1980 from http://www.freepatentsonline.com/

Puduki M, Yaakob Z (2014) Catalytic aspects of ceria zirconia solid solution: part II. An overview on recent developments in the heterogenous catalytic application of metal loaded ceria-zirconia solid solution. Der Pharma Chem 6(1):224–240

Rahman FA, Aziz MMA, Saidur R, Wan Abu Bakar WA, Hainin MR, Putrajaya R, Hassan NA (2017) Pollution to solution: capture and sequestration of carbon dioxide (CO_2) and its utilization as a renewable energy source for a sustainable future. Renew Sust Energ Rev 71:112–126

Ramaroson E, Tempere JF, Guilleux MF (1992) Spectroscopic characterization and reactivity study of ceria-supported nickel catalysts. J Chem Soc Faraday Transact 88(8):1211–1218

Rao GR, Mishra BG (2003) Structural, redox and catalytic chemistry of ceria based materials. Bull Catal Soc India 2:122–134

Razzaq R, Zhu HW, Jiang L, Muhammad U, Li C, Zhang S (2013) Catalytic methanation of CO and CO_2 in coke oven gas over Ni-Co/ZrO_2-CeO_2. Ind Eng Chem Res 52:2247–2256

Riboldi L, Bolland O (2017) Overview on pressure swing adsorption (PSA) as CO_2 capture technology: state of the art, limits and potentials. Energy Procedia 114(2390):2400

Rosid SJM, Abu Bakar WAW, Ali R (2013) Methanation reaction over samarium oxide based catalysts. Malaysian J Fundament Appl Sci 9(1):28–34

Rosid SJM, Abu Bakar WAW, Ali R (2015a) Catalytic CO_2/H_2 methanation reaction over alumina supported manganese/cerium oxide based catalysts. Adv Mater Res 1107:67–72

Rosid SJM, Bakar WAWA, Ali R (2015b) Physicochemical study of supported cobalt–lanthanum oxide-based catalysts for CO_2/H_2 methanation reaction. Clean Techn Environ Policy 17(1):257–264

Rosid SJ, Wan Abu Bakar WA, Ali R (2015c) Optimization of praseodymium oxide based catalysts for methanation reaction of simulated natural gas using Box-Behnken design. Jurnal Teknologi 75(1):55–65

Rosid SJM, Abu Bakar WAW, Ali R (2018) Characterization and modelling optimization on methanation activity using Box-Behnken design through cerium doped catalysts. J Clean Prod 170:278–287

Rosid SJM, Abu Bakar WAW, Toemen S, Yusoff NM, Azid A, Mokhtar WNAW (2019a) Investigation of active species in methanation reaction over cerium based loading. Malaysian Journal of Fundamental and Applied Sciences. Special Issue on International Conference on Agriculture, Animal Sciences and Food Technology (ICAFT 2018b) 319–323

Rosid SJM, Toemen S, Abu Bakar WAW, Zamani AH, Mokhtar WNAW (2019b) Physicochemical characteristic of neodymium oxide-based catalyst for in-situ CO_2/H_2 methanation reaction. J Saudi Cheml Soc 23:284–293

Ruiz P, Jacquemin M, Blangenois N (2009) Patentscope W02010006386 A2. Retrieved on September 15, 2009 from http://www.freepatentsonline.com/

Rynkowski J, Farbotko J, Touroude R, Hilaire L (2000) Redox behavior of ceria titania mixed oxide. Appl Catal A: General 203:335–348

Sahki R, Benlounes O, Chérifi O, Thouvenot R, Bettahar MM, Hocine S (2011) Effect of pressure on the mechanisms of the CO_2/H_2 reaction on a CO-precipitated $CuO/ZnO/Al_2O_3$ catalyst. React Kinet Mech Catal 103(2):391–403

Saluko AE (2005) Removal of carbon dioxide from natural gas for LNG production. Institute of Petroleum Technology Norwegian University of Science and Technology

Schaper H, Doesburg EBM, Van Reijen LL (1985) Thermal stabilization of high surface area alumina. Appl Catal 14:371

Scholten SA, Allison JD, Dunn BC (2012) United States Patent 8754137 B2. Retrieved on March 15, 2012 from http://www.freepatentsonline.com/

Sehested J, Dahl S, Jacobsen J, Rostrup-Niclsen JR (2004) Methanation of CO over nickel: mechanism and kinetic at high H_2/CO ratios. J Phys Chem B 109(6):2432–2438

Seiyama T (1992) Total oxidation of hydrocarbons on perovskite oxides. Catal Rev Sci Eng 34(4):280–300

Sharma S, Hu Z, Zhang P, McFarland EW, Metiu H (2011) CO_2 methanation on Ru-doped ceria. J Catal 278:297–309

Sharma S, Sravan Kumar KB, Chandnani YM, Phani Kumar VS, Gangwar BP, Singhal A, Deshpande PA (2016) Mechanistic insights into CO_2 methanation over Ru-substituted CeO_2. J Phys Chem C 120(26):14101–14112

Silva DCDD, Letichevsky S, Borges LEP, Appel LG (2012) Catalyst and the methanation of CO and CO_2. Int J Hydrog Energy 37(11):8923–8928

Sims CM, Maier RA, Johnston-Peck AC, Gorham JM, Hackley VA, Nelson BC (2019) Approaches for the quantitative analysis of oxidation state in cerium oxide nanomaterials. Nanotechnology 30. 085703:1–14

Solarin SA, Ozturk I (2016) The relationship between natural gas consumption and economic growth OPEC members. Renew Sust Energ Rev 58:1348–1356

Solymosi F, Erdehelyi A, Bansagi T (1981) Methanation of CO_2 on supported rhodium catalyst. J Catal 68:371–382

Song H, Yang J, Zhao J, Chou L (2010) Methanation of carbon dioxide over a highly dispersed Ni/La_2O_3 catalyst. Chin J Catal 31:21–33

Speight JG (2007) Natural gas: a basic handbook. Gulf Publishing Company, Houston

Stevens RW, Siriwardane RV, Logan J (2008) In situ Fourier transform infrared (FTIR) investigation of CO_2 adsorption onto zeolite materials. Energy Fuel 22:3070–3079

Stookey DJ, Patton CJ, Malcolm GL (1986) Membranes separate gases selectively. CEP, pp. 36–40

Strakey JP, Forney AJ, Haynes WP (1975) Department of Commerce National Technical Information Service. Energy Research and Development Administration, Pittsburgh PA. Pittsburgh Energy Centre

Su BL, Guo SD (1999) Effects of rare earth oxides on stability of Ni/α-Al_2O_3 catalysts for steam reforming of methane. Stud Surf Sci Catal 126:325–332

Sudhanshu S, Zhenpeng H, Peng Z, Eric WM, Horia M (2011) CO_2 methanation on Ru-doped ceria. J Catal 278:297–309

Tada S, Shimizu T, Kameyama H, Haneda T, Kikuchi R (2012) Ni/CeO_2 catalysts with high CO_2 methanation activity and high CH_4 selectivity at low temperatures. Int J Hydrog Energy 37(7):5527–5531

Tada S, Ochieng OJ, Kikuchi R, Hanada T, Kameyama H (2014) Promotion of CO_2 methanation activity and CH_4 selectivity at low temperature over $Ru/CeO_2/Al_2O_3$ catalysts. Int J Hydrog Energy 39(19):10090–10100

Tang X, Li Y, Huang X, Xu Y, Zhu H, Wang J, Shen W (2006) MnO_x–CeO_2 mixed oxide catalysts for complete oxidation of formaldehyde: effect of preparation method and calcination temperature. Appl Catal B Environ 62(3–4):265–273

Toemen S, Wan Abu Bakar WA, Ali R (2014) Copper/nickel/manganese doped cerium oxides based catalysts for hydrogenation of CO_2. Bull Kor Chem Soc 35(8):2349

Toemen S, Wan Abu Bakar WA, Ali R (2016) Effect of ceria and strontia over $Ru/Mn/Al_2O_3$ catalyst: catalytic methanation, physicochemical and mechanistic studies. J CO2 Util 13:38–49

Vicente MA, Belver C, Trujillano R, Rives V, Alvarez AC, Lambert JF, Korili SA, Gandia LM, Gil A (2004) Preparation and characterization of Mn- and Co-supported catalysts derived from Al-pillared clays and Mn- and Co-complexes. Appl Catal A Gen 267:47–58

Bakar WAWA, Othman MY, Ali R, Yong CK, Toemen S (2009) The investigation of active sites on nickel oxide based catalysts towards the in-situ reactions of methanation and desulfurization. Mod Appl Sci 3:36–44

Bakar WAWA, Ali R, Mohammad NS (2015) The effect of noble metals on catalytic methanation reaction over supported Mn/Ni oxide based catalysts. Arab J Chem 8:632–643

Wang A, Lu GQ (1998) Reforming of methane with carbon dioxide over Ni/Al_2O_3 catalyst: effect of nickel precursor. Appl Catal A: General 169:271–280

Wang F, He S, Chen H, Wang B, Zheng L, Wei M, Evans DG, Duan X (2016) Active site dependent reaction mechanism over Ru/CeO_2 catalyst towards CO_2 methanation. J Am Chem Soc 138:6298–6305

Wierzbicki D, Debek R, Motak M, Grzybek T, Galvez ME, Da Costa P (2016) Novel Ni-La hydrotalcite derived catalysts for CO_2 methanation. Catal Commun 83:5–8

William EL, David ER (2005) Natural gas composition. Gas Technology Institute

Wood CD, Gleason EF (1987) United States Patent 4666881. Retrieved on, May 19, 1987 from http://www.freepatentsonline.com/

Xavier KO, Sreekala RK, Rashid KA, Yusuff KKM, Sen B (1999) Doping effects of cerium oxide on Ni/Al_2O_3 catalysts for methanation. Catal Today 49:17–21

Xu XY, Lin JJ, Hao ZP (2006) CeO_2-Co_3O_4 catalysts for CO oxidation. J Rare Earths 24:172–176

Zamani AH, Ali R, Bakar WAWA (2014) The investigation of Ru/Mn/Cu-Al_2O_3 oxide catalysts for CO_2/H_2 methanation in natural gas. J Taiwan Inst Chem Eng 45(1):143–152

Zamani AH, Ali R, Bakar WAWA (2015a) Optimization of CO_2 methanation reaction over M*/Mn/Cu–Al_2O_3 (M*: Pd, Rh and Ru) catalysts. J Ind Eng Chem 29:238–248

Zamani AH, Ali R, Bakar WAWA (2015b) CO_2/H_2 methanation over M*/Mn/Fe-Al_2O_3 (M*: Pd, Rh, and Ru) catalysts in natural gas; optimization by response surface methodology-central composite design. Clean Techn Environ Policy 17(3):627–636

Zhi G, Guo X, Wang Y, Jin G, Guo X (2011) Effect of La_2O_3 modification on the catalytic performance of Ni/SiC for methanation of carbon dioxide. Catal Commun 16(1):56–59

Zuo M, Zhuang S, Tan X, Meng B, Yang N, Liu S (2014) Ionic conducting ceramic-carbonate dual phase hollow fibre membranes for high temperature carbon dioxide separation. J Membr Sci 458: 58–65